fructose:glucose ratio would be 75:25, better than the ratio used commercially.

Finally, some minor alterations could further improve the productivity of the process. First, the cycle time (3–6 h) of the semicontinuous process using transaldolase was longer than necessary for optimal productivity. Second, higher amounts of phosphoglycerate phosphatase (the rate-limiting enzyme) would improve productivity. Finally, concentrations of glyceraldehyde used were much greater than the K_M of the transaldolase. As the transaldolase-catalyzed step is not rate limiting, the amount of glyceraldehyde could be reduced substantially without greatly influencing the rate of production of fructose.

(37) Hestrin, S. *J. Biol. Chem.* **1949**, *179*, 943.
(38) Colowick, S. P.; Sutherland, E. W. *J. Biol. Chem.* **1942**, *144*, 423.
(39) Robinson, W. G. *Methods Enzymol.* **1966**, *9*, 332.

Registry No. ATPase, 9000-83-3; DNase I, 9003-98-9; G6P, 56-73-5; G1P, 59-56-3; F6P, 643-13-0; THF, 109-99-9; MeOH, 67-56-1; EtOH, 64-17-5; fructose, 57-48-7; starch, 9005-25-8; glucose-6-phosphate dehydrogenase, 9001-40-5; glucose oxidase, 9001-37-0; peroxidase, 9003-99-0; phosphoglucose isomerase, 9001-41-6; pyruvate kinase, 9001-59-6; lactate dehydrogenase, 9001-60-9; phosphorylase *a*, 9032-10-4; phosphoglucomutase, 9001-81-4; fructose dehydrogenase, 37250-85-4; transaldolase, 9014-46-4; sorbitol dehydrogenase, 9028-21-1; lysozyme, 9001-63-2; phosphofructokinase, 9001-80-3; 3-phosphoglycerate phosphatase, 62213-13-2; fructose kinase, 9030-51-7; 5′-nucleotidase, 9027-73-0; D-glyceraldehyde, 453-17-8; glucose, 50-99-7; glycerol kinase, 9030-66-4; fructose 6-phosphatase, 76774-41-9; pyridine, 110-86-1; 1*H*-imidazole, 288-32-4; 2,6-lutidine, 108-48-5; 1,4-dioxane, 123-91-1; 3-phosphoglycerate, 820-11-1; glyceraldehyde 3-phosphate, 142-10-9.

Calculated and Experimental Absolute Stereochemistry of the Styrene and β-Methylstyrene Epoxides Formed by Cytochrome $P450_{cam}$

Julia A. Fruetel,[†] Jack R. Collins,*[,‡] Debra L. Camper,[‡] Gilda H. Loew,*[,‡] and Paul R. Ortiz de Montellano*[,†]

Contribution from the Department of Pharmaceutical Chemistry, School of Pharmacy, University of California, San Francisco, California 94143-0446, and Molecular Research Institute, 845 Page Mill Road, Palo Alto, California 94304. *Received January 31, 1992*

Abstract: Cytochrome $P450_{cam}$ oxidizes styrene to styrene oxide and a trace of phenylacetaldehyde; *cis*-β-methylstyrene to *cis*-β-methylstyrene oxide, *cis*-3-phenyl-2-propen-1-ol, and a trace of 1-phenyl-2-propanone; and *trans*-β-methylstyrene to *trans*-β-methylstyrene oxide, *trans*-3-phenyl-2-propen-1-ol, and a trace of 1-phenyl-2-propanone. Aromatic ring hydroxylation is also observed as a very minor process with each of the three substrates. Benzaldehyde is formed as a major product in all the reactions, but its formation is due to oxidation of the olefins by the H_2O_2 produced by uncoupled turnover of the enzyme. Stoichiometry studies indicate that oxidation of the styrenes is highly uncoupled relative to the oxidation of camphor. Analysis of the absolute stereochemistry of the three epoxides by chiral gas–liquid chromatography shows that the stereoisomers are formed in the following ratios: styrene oxide, *S*:*R* 83:17; *cis*-β-methylstyrene oxide, 1*S*,2*R*:1*R*,2*S* 89:11; *trans*-β-methylstyrene oxide, 1*S*,2*S*:1*R*,2*R* 75:25. Calculation of the minimum energy conformations of the three olefins, docking of the preferred conformations in the active site of cytochrome $P450_{cam}$ with use of AMBER to calculate the minimum energy orientations, and molecular dynamic simulations independently predict the following epoxide stereoisomer ratios: styrene oxide, *S*:*R* 65:35; *cis*-β-methylstyrene oxide, 1*S*,2*R*:1*R*,2*S* 84:16; *trans*-β-methylstyrene oxide, 1*S*,2*S*:1*R*,2*R* 75:25. The excellent agreement between theory and experiment supports the validity of the computational methodology and provides insight into the factors that control the stereoselectivity and outcome of cytochrome P450-catalyzed oxidations.

Cytochrome P450 enzymes play critical roles in the biosynthesis and metabolism of the steroids, fatty acids, eicosanoids, and other lipophilic endobiotics.[1-3] They also catalyze the oxidation of drugs and xenobiotics to more polar, more readily excreted, and sometimes more toxic metabolites.[1,4,5] Despite their biosynthetic and catabolic importance, little information is available on the active sites of these enzymes except for cytochrome $P450_{cam}$, a cytosolic enzyme from *Pseudomonas putida* that catalyzes the 5-hydroxylation of camphor.[6] The crystal structure of this enzyme, which has been solved in the presence and absence of camphor to a resolution of 1.6 and 2.2 Å, respectively,[7,8] currently serves as the template for all efforts to model the active sites of other cytochrome P450 enzymes. Analysis of the substrate-bound crystal structure suggests that hydrogen bonding of the camphor oxygen to Tyr 96 and interaction of its methyl groups with Val 295 and Val 247 are primarily responsible for orienting the substrate in the active site and promoting its regio- and stereospecific hydroxylation.[7-9] Experimental support for the primacy of these interactions is provided by the fact that site-specific replacement of Tyr 96 by a phenylalanine or either of the two valines by an isoleucine decreases the regio- and stereospecificity of camphor hydroxylation.[10,11] Conversely, replacement of the camphor oxygen by a sulfur, yielding a much poorer hydrogen bond acceptor with a great mobility in the active site, also results

* Authors to whom correspondence should be addressed.
[†] University of California, San Francisco.
[‡] Molecular Research Institute.

(1) *Cytochrome P450: Structure, Mechanism, and Biochemistry*; Ortiz de Montellano, P. R., Ed.; Plenum Press: New York, 1986.
(2) Gonzalez, F. J. *Pharmacol. Ther.* **1990**, *45*, 1.
(3) Kupfer, D. *Pharmacol. Ther.* **1980**, *11*, 469.
(4) Yang, C. S.; Lu, A. Y. H. In *Mammalian Cytochromes P450*; Guengerich, F. P., Ed.; CRC Press: Boca Raton, FL, 1987; Vol. 2, pp 1–17.
(5) Nelson, S. D.; Harvison, P. J. In *Mammalian Cytochromes P450*; Guengerich, F. P., Ed.; CRC Press: Boca Raton, FL, 1987; Vol. 2, pp 19–79.
(6) Sligar, S. G.; Murray, R. I. In *Cytochrome P450: Structure, Mechanism, and Biochemistry*; Ortiz de Montellano, P. R., Ed.; Plenum Press: New York, 1986; p 429–503.
(7) Poulos, T. L.; Finzel, B. C.; Howard, A. J. *J. Mol. Biol.* **1987**, *195*, 687.
(8) Poulos, T. L.; Finzel, B. C.; Howard, A. J. *J. Biochemistry* **1986**, *25*, 5314.
(9) Poulos, T. L.; Finzel, B. C.; Gunsalus, E. C.; Wagner, G. C.; Kraut, J. *J. Biol. Chem.* **1985**, *260*, 16122.
(10) Atkins, W. M.; Sligar, S. G. *J. Biol. Chem.* **1988**, *263*, 18842.
(11) Atkins, W. M.; Sligar, S. G. *J. Am. Chem. Soc.* **1989**, *111*, 2715.

0002-7863/92/1514-6987$03.00/0

in a loosening of the hydroxylation specificity.[12,13] Although cytochrome $P450_{cam}$ has generally been considered to be a substrate-specific enzyme, it has been shown to oxidize closely related structures such as norcamphor, 5,5-difluorocamphor, pericyclocamphanone, adamantanone, adamantane, and 5,6-dehydrocamphor.[14] Force field and heat of formation calculations have predicted oxidation results for some of these analogues in good agreement with the experimental data.[15] Recent work has shown that cytochrome $P450_{cam}$ also oxidizes completely unrelated substrates. In preliminary communications, we reported that the enzyme epoxidizes *cis*-β-methylstyrene,[16] and another group reported the oxidation of a tetralone.[17] The finding that cytochrome $P450_{cam}$ oxidizes xenobiotics for which the active site has not been specifically tailored led us to explore the feasibility of utilizing computational methods to predict the reaction stereochemistry for oxidations that are primarily controlled by steric and hydrophobic interactions within a well-defined protein structure. An understanding of the parameters that control the specificity of such reactions is critical to efforts to predict the roles of individual isozymes in drug and xenobiotic metabolism, to the development of isozyme-specific inhibitors, and to the targeted modification by site specific mutagenesis of substrate specificity.

Experimental Section

Enzymes. Cytochrome $P450_{cam}$, putidaredoxin, and putidaredoxin reductase were purified essentially as described before.[18] Camphor-free cytochrome $P450_{cam}$ was prepared immediately before use by preincubation with ~10 mM dithiothreitol for 10 min at room temperature followed by passage over a Sephadex G-15 column equilibrated with 50 mM potassium phosphate buffer (pH 7.0). Spectra taken of the protein after the column consistently showed no shoulder at 391 nm, indicating no residual bound camphor. The β-mercaptoethanol in the stock putidaredoxin solution was removed for the hydrogen peroxide assays by passage of the enzyme immediately before it was used through a G-15 column equilibrated in 50 mM Tris·HCl buffer (pH 7.4).

Chemicals. Styrene, styrene oxide, (*R*)-styrene oxide, *trans*-β-methylstyrene, (1*R*,2*R*)-(+)-1-phenylpropylene oxide, (1*S*,2*S*)-(−)-1-phenylpropylene oxide, and (1*R*)-(+)-camphor were purchased from Aldrich Chemical Co. Bis(trimethylsilyl)trifluoroacetamide (BSTFA), DL-dithiothreitol, and NADH were purchased from Sigma. *cis*-β-Methylstyrene was purchased from K&K Laboratories. Ammonium thiocyanate and ferrous ammonium sulfate were purchased from Fisher. A 70:30 mixture of (1*S*,2*R*)-(+)-1-phenylpropylene oxide and (1*R*,2*S*)-(−)-1-phenylpropylene oxide, respectively, was kindly provided by Dr. Thomas Kodadek (University of Texas, Austin).[19] The 5-*exo*-hydroxycamphor standard was a gift from Dr. Julian A. Peterson (University of Texas Health Sciences Center, Dallas). All chemicals were used without further purification except for the olefins, which were purified by silica gel chromatography with pentane as the eluting solvent immediately before each experiment.

Gas–liquid chromatography was carried out on a Hewlett Packard Model 5890A gas chromatograph equipped with a flame ionization detector and a Hewlett Packard 3390A integrator. High-pressure liquid chromatography was performed on a system consisting of a Hewlett Packard 9153C controller, a Hewlett Packard diode-array detector, and two Beckman Model 110A pumps. Mass spectra were obtained on a VG-70 mass spectrometer equipped with a Hewlett Packard 5890A gas chromatograph.

Metabolite Formation, Identification, and Quantitation. Incubations containing 50 mM potassium phosphate buffer (pH 7.0), 2 mM substrate, 1 μM cytochrome $P450_{cam}$, 8 μM putidaredoxin, 2 μM putidaredoxin reductase, and 0.8 mM EDTA were preincubated for 2 min at 25 °C in a shaking water bath. NADH (1 mM final concentration) or buffer (in control experiments) was then added to start the incubation. In incubations with camphor as the substrate, the NADH concentration was increased to 5 mM.

To quantitate each of the olefin metabolites, 1-mL aliquots were removed from the incubation mixture at designated time points (for the *cis*- and *trans*-cinnamyl alcohols, 3-mL aliquots were required for accurate quantitation). A solution of the internal standard in methanol was immediately added, and the aliquot was extracted with 0.5 mL of CH_2Cl_2. The CH_2Cl_2 layer was analyzed before and after derivation with BSTFA by gas–liquid chromatography on a DB-1 fused silica capillary column (0.25 mm i.d. × 30 m). The column temperature was programmed to hold at 45 °C for 2 min and then to rise 4°/min to 140 °C. Derivatization with BSTFA was required to detect and quantitate the alcohol metabolites. The metabolites were quantitated using standard curves with *R*-styrene oxide as the internal standard for the *cis*- and *trans*-β-methylstyrene incubations and (1*S*,2*S*)-1-phenylpropylene oxide for the styrene incubations. The retention times of the components were the following: styrene, 6.8 min; benzaldehyde, 8.9 min; phenylacetaldehyde, 11.3 min; styrene oxide, 12.7 min; *cis*-β-methylstyrene, 10.0 min; *cis*-β-methylstyrene oxide, 14.1 min; phenylacetone, 15.0 min; *cis*-cinnamyl alcohol (+BSTFA), 23.5 min; *trans*-β-methylstyrene, 11.3 min; *trans*-β-methylstyrene oxide, 14.6 min; *trans*-cinnamyl alcohol (+BSTFA), 25.8 min. The identity of each of the metabolites was established by coelution with authentic standards and by gas–liquid chromatography/electron impact mass spectrometry.

To quantitate the 5-*exo*-hydroxycamphor formed from *d*-camphor, 0.1-mL aliquots were removed from the incubations and the aliquots were added to 0.9 mL of double glass-distilled water containing the internal standard 1-adamantanol. This was extracted with 0.5 mL of diethyl ether, the extract was derivatized with BSTFA, and the derivatized sample was analyzed by gas–liquid chromatography on a DB-1 capillary column. The column temperature was programmed to hold at 85 °C for 2 min and then to rise 4°/min to 140 °C and then 9°/min to 185 °C. The retention times of the components are as follows: *d*-camphor; 8.1 min; 1-adamantanol (+BSTFA), 11.0 min; 5-*exo*-hydroxycamphor (+BSTFA), 13.7 min. The amount of metabolite formed was quantitated by using standard curves based on extraction of the hydroxylated camphor and 1-adamantanol standard from the complete incubation system (incorrect values are obtained if the standards are extracted from mixtures without the protein).

Epoxidation Stereochemistry. The ratio of the epoxide enantiomers was determined by first purifying the epoxide metabolite by normal phase HPLC and then analyzing it by chiral phase gas–liquid chromatography. The isocratic HPLC purification was carried out on an Alltech Partisil Silica 5-μm column eluted with 2.5% THF in hexane at 1 mL/min. The eluent was monitored at 260 nm. A 1-mL 30-min incubation of the olefin with the cytochrome $P450_{cam}$ system was extracted with 0.5 mL of hexane and as much as possible of the hexane layer (0.2–0.3 mL) was injected onto the HPLC column. The epoxide metabolite was collected (retention time = 7–8 min for the styrene and β-methylstyrene epoxides) and the sample concentrated and injected onto a Chiraldex G-TA capillary column (0.25 mm i.d. × 30 m, Advanced Separation Technologies Inc.) at 76 °C. The retention times of the epoxide enantiomers were the following: (*S*)-(−)-styrene oxide, 9.8 min; (*R*)-(+)-styrene oxide, 10.9 min; (1*S*,2*R*)-(+)-1-phenylpropylene oxide, 9.7 min; (1*R*,2*S*)-(−)-1-phenylpropylene oxide, 11.9 min; (1*S*,2*S*)-(−)-1-phenylpropylene oxide, 10.1 min; (1*R*,2*R*)-(+)-1-phenylpropylene oxide, 11.2 min.

Oxygen Consumption. The rate of oxygen consumption by cytochrome $P450_{cam}$ was measured by using a Clark electrode with the cell connected to a constant temperature bath set at 27 °C. The incubation mixture (1.3 mL) was placed inside the cell and allowed to equilibrate 5 min or until the oxygen level had stabilized. The reaction was initiated by the addition of NADH, and the loss of oxygen was monitored until it leveled off. The rate of oxygen consumed was determined as the initial rate over the first 2 min, with a full-scale deflection corresponding to an oxygen concentration of 232 μM. When the amount of NADH was increased to 5 mM, the loss of oxygen was linear and went to completion.

NADH Consumption. The rate of NADH utilization by cytochrome $P450_{cam}$ was determined spectrophotometrically. Aliquots (0.2 mL for the olefin incubations, 0.05 mL for the camphor incubations) were removed from the incubation mixture at various time points and diluted to 1 mL in a cuvette, and the absorbance at 340 nm was immediately measured. The amount of NADH consumed was quantitated by using the extinction coefficient $\epsilon = 6.22\ mM^{-1}\ cm^{-1}$.

Hydrogen Peroxide Formation. The amount of hydrogen peroxide formed by cytochrome $P450_{cam}$ was measured with use of an iron(II) thiocyanate assay.[20] Accurate measurements with this assay require

(12) Atkins, W. M.; Sligar, S. G. *J. Biol. Chem.* **1988**, *263*, 18842.
(13) Raag, R.; Poulos, T. L. *Biochemistry* **1991**, *30*, 2674.
(14) (a) White, R. E.; McCarthy, M. B.; Egeberg, K. D.; Sligar, S. G. *Arch. Biochem. Biophys.* **1984**, *228*, 493. (b) Eble, K. S.; Dawson, J. H. *J. Biol. Chem.* **1984**, *259*, 14389. (c) Gelb, M. H.; Malkonen, P.; Sligar, S. G. *Biochem. Biophys. Res. Commun.* **1982**, *104*, 853.
(15) Collins, J. R.; Loew, G. H. *J. Biol. Chem.* **1988**, *263*, 3164.
(16) Ortiz de Montellano, P. R.; Fruetel, J. A.; Collins, J. R.; Camper, D. L.; Loew, G. H. *J. Am. Chem. Soc.* **1991**, *113*, 3195.
(17) Watanabe, Y.; Ishimura, Y. *J. Am. Chem. Soc.* **1989**, *111*, 410.
(18) Gunsalus, I. C.; Wagner, G. C. In *Methods in Enzymology*; Fleischer, S., Packer, L., Eds.; Academic Press: New York, 1978; Vol. 52, Part C, pp 166–188.
(19) O'Malley, S.; Kodadek, T. *J. Am. Chem. Soc.* **1989**, *111*, 9116.
(20) Colorimetric Determination of Nonmetals. *Chemical Analysis*; Boltz, D. F., Howell, J. A., Eds.; Wiley and Sons: New York, 1978; Vol. 8, pp 305–306.

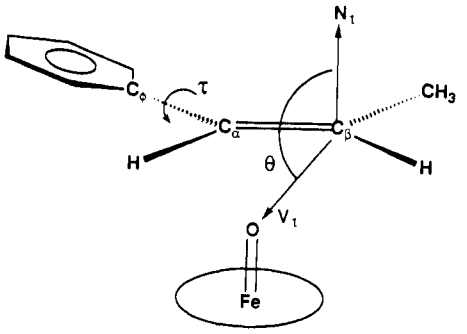

Figure 1. The vectors (N_1 and V_1) used to calculate the angle θ that discriminates between the two faces of the π-bond, corresponding to the different enantiomeric products, are shown. τ is the dihedral angle relating the plane of the phenyl ring and the allyl moiety. The magnitude of the vector V_1 was used to determine which orientations were within the 4 Å cutoff distance.

EDTA-free buffers. Aliquots (0.3 mL) were removed from the incubation mixture at various time points and added to 0.2 mL of 0.3 N sulfuric acid kept on ice. To this was then added 0.125 mL of a 6 mM ferrous ammonium sulfate solution, 0.125 mL of a 6 M ammonium thiocyanate solution, and 0.75 mL of deionized, doubly-distilled water. The mixture was then centrifuged for 1 min to pellet the precipitated protein, and the absorbance at 480 nm was measured. The amount of hydrogen peroxide present was calculated from a standard curve made with a stock hydrogen peroxide solution.

Calculated Conformations of Styrene, *cis*-β-Methylstyrene, and *trans*-β-Methylstyrene. The geometries of styrene, *cis*-β-methylstyrene, and *trans*-β-methylstyrene were first optimized with use of the AM1 method as implemented in the program MOPAC (5.0).[21] The optimized geometries were then used for templates in the molecular mechanics calculations. Parameters that resulted in AMBER minimized geometries consistent with the AM1 calculations for these three substrates were then added to the AMBER parameter list and are listed in Table I.[22] The partial charges used in the AMBER calculations, also listed in Table I, were taken from the AM1 Mulliken population analysis.

Epoxide Intermediate Formation. The stabilities of the radicals formed by addition of OH radical to the C_α and C_β atoms of *cis*-β-methylstyrene were calculated with the AM1 Hamiltonian and the UHF method for open shell doublets. Four optimized geometries, formed by attack of OH radical at both C_α and C_β for each face, were used to determine the radical stabilities. This information was later used to develop the mechanism-based criteria for analysis of the MD simulations. When describing the geometries of the individual substrates and particular carbon atoms for oxygen attack, we use the nomenclature of "α" and "β" to distinguish the atoms (see Figure 1). However, when later describing the stereospecific epoxide products, we denote the enantiomers as 1*S*,2*R* etc. where the "1" and "2" refer to the stereochemistry about the "α" and "β" carbons, respectively.

Enzyme–Substrate Interactions. To model the enzyme–substrate interactions of styrene, *cis*-β-methylstyrene and *trans*-β-methylstyrene with cytochrome P450, we used the binding site of cytochrome $P450_{cam}$ from the crystal structure of the adamantanone bound enzyme, as in previous publications.[24,28] This binding site includes 87 amino acids, extending approximately 12 Å from the center of the heme unit, as well as 7 bound water molecules from the crystal structure and the protoporphyrin IX heme unit. The heme unit included the putative, biologically active, ferryl-oxo atom. In the ferryl–oxo model, an oxygen atom is placed perpendicular to the porphyrin plane opposite from the cysteinate ligand at a distance of 1.7 Å from the Fe atom, a value consistent with that obtained for the ferryl–oxo complex of peroxidases from EXAFS studies.[23] The parameters and charges for the ferryl–oxo model were taken from previous AMBER[24] calculations using this model.

Substrate Docking. With use of the program MIDAS, styrene was placed in the binding site of cytochrome $P450_{cam}$ in two orientations ("O1" and "O2"). In the first orientation (O1), the face leading to the 1*S* epoxide product was directed toward the ferryl oxygen, while in the second (O2), the face leading to the 1*R* epoxide was directed toward the oxygen.

cis-β-Methylstyrene was docked into the binding site of cytochrome $P450_{cam}$ in four (4) orientations ("O1", "O2", "O3", and "O4"), again using MIDAS. Two rotamers about the C_ϕ–C_α dihedral angle, corresponding to 40° and −40°, were used for the docking. Qualitatively, the orientation of the phenyl group with respect to the allylic moiety is different for the two different conformations in the protein and could lead to different stereospecificity of the epoxide products. These rotamers (+40° and −40°) were each docked in two orientations such that the face leading to the 1*S*,2*R* epoxide would be directed toward the ferryl oxygen in the first and the 1*R*,2*S* in the second.

As with the *cis* conformer, *trans*-β-methylstyrene was docked into the binding site of cytochrome $P450_{cam}$ in four orientations ("O1", "O2", "O3", and "O4"), using MIDAS. The 1*S*,2*S* and 1*R*,2*R* faces, respectively, were oriented toward the ferryl oxygen in the first two dockings. Since the *trans* conformer of β-methylstyrene is planar, the substrate conformation was kept fixed in all dockings. A rigid rotation about an axis containing the center of the phenyl ring and the C_α atom of the substrate resulted in two additional orientations of the substrate, differing from the initial dockings with respect to the nearby amino acids of the protein. This rotation resulted in another pair of orientations, with 1*S*,2*S* and 1*R*,2*R* faces, respectively, directed toward the ferryl oxygen.

In all of the docked orientations, the phenyl ring was directed away from the ferryl oxygen. It was assumed that the oxygen attack leading to epoxide formation would be along the π system of the allylic double bond, perpendicular to the plane of the allyl system. Each docked orientation was energy minimized with use of AMBER (3.0A).

Table I. Parameters Used in AMBER Calculations for Styrene and *cis*- and *trans*-β-Methylstyrene

Styrene Charges Taken from AM1 Mulliken Populations

atom	charge	atom	charge
C1–5,7	−0.10	C6	−0.05
C8	−0.15	Hs	0.10

trans- and *cis*-β-Methylstyrene Charges Taken from AM1 Mulliken Populations

atom	charge	atom	charge
C1–5	−0.13	H1–5	0.136
C6	−0.04		
C7,8	−0.14	H7,8	0.12
C9	−0.19	H9s	0.08

Bond Parameters Added to AMBER for Styrene and β-Methyl Analogues

	k	*r*		*k*	*r*
C6–7	450	1.50	C7–H	450	1.09
C7–C8	450	1.35	C8–H	450	1.09
C8–C9	450	1.47			

Angle Parameters Added to AMBER for Styrene and Analogues

	k	φ		*k*	φ
Cφ–C6–C7	70.0	120.0	H–C7–C8	60.0	120.0
C6–C7–C8	50.0	120.0	C7–C8–C9	70.0	120.0
C7–C8–H	50.0	120.0	C8–C9–H	70.0	109.47
C6–C7–H	50.0	120.0	H–C8–C9	70.0	120.0
H–C8–H	50.0	120.0			

Dihedral Parameters Added to AMBER for Styrene and Analogues

	k	φ	*a*	*b*
X–Cφ–C7–X	1.6	180.0	2	2
X–C7–C8–X	3.0	180.0	2	2
HX–C8–CT–HC	0.5	180.0	2	3
X–Cφ–C7–X[a]	3.2	180.0	2	2
X–C7–C8–X[a]	15.0	180.0	2	2

Nonbonded Parameters Added to AMBER for Styrene and Analogues

	k	*r*
C7	0.12	1.85
C8	0.12	1.93

[a] Alternative values used in a second simulation of styrene.

(21) Dewar, M. S. J.; Zoebisch, E. G.; Healy, E. F.; Stewart, J. J. P. *J. Am. Chem. Soc.* **1985**, *107*, 3902.
(22) Singh, U. C.; Weiner, P. K.; Caldwell, J. W.; Kollman, P. A. AMBER UCSF Version 3.0a, Department of Pharmaceutical Chemistry, University of California, San Francisco, 1986; Revision A by George Seibel, 1989.
(23) Chance, B.; Powers, L.; Ching, Y.; Poulos, T.; Schonbaum, G. R.; Yamazaki, I.; Paul, K. G. *Arch. Biochem. Biophys.* **1984**, *235*, 596.
(24) Collins, J. R.; Camper, D. L.; Loew, G. H. *J. Am. Chem. Soc.* **1991**, *113*, 2736.

All minimizations were performed with a constant dielectric of 1.0 and a 9.0 Å cutoff distance for nonbonded interactions. The minimizations were considered to be converged when the RMS gradient fell below 0.1. Because the 87 amino acids forming the extended substrate binding site were not contiguous in the protein, the backbone (N,C_α,C) atoms were constrained in coordinate space by using a harmonic potential of 100 kcal/Å^2 in all of the molecular mechanics calculations. All side chain, porphyrin, and substrate molecules were allowed to move freely. Net intermolecular energies between the protein binding site and the substrate were calculated with the ANAL program from AMBER.

Substrate–Protein Dynamics. Molecular dynamics (MD) calculations were also performed with the program AMBER (3.0A), starting from the minimized orientations: two for styrene, four for *cis*-β-methylstyrene, and four for *trans*-β-methylstyrene. Two initial Maxwellian velocity distributions (designated "V1" and "V2", respectively) generated from two random number seeds corresponding to 298 K were used for each minimized complex. This combination of optimized initial complex geometries and initial velocity distributions resulted in 4, 8, and 8 initial conditions and corresponding trajectories from them for styrene, *cis*-β-methylstyrene, and *trans*-β-methylstyrene, respectively. All bonds were constrained with the SHAKE algorithm. The simulations employed a nonbond cutoff of 9 Å with the nonbonded pairlist updated every 25 steps. Electrostatic interactions were modeled using a distance-dependent dielectric constant. The integration time step was 0.001 ps. Five picoseconds (5 ps) of MD were first performed for each orientation to allow for heating and equilibration of the systems. Constant temperature (298 K with a tolerance of 12 K and a coupling constant of 0.1 ps) MD trajectories of 125 ps followed each heating and equilibration run with coordinate sets saved every 0.2 ps, resulting in 625 coordinate sets per trajectory. In addition to the backbone atoms, the oxygen atoms of the water molecules were also constrained by using a harmonic potential with the same force constant as in the minimization steps. Molecular dynamics simulations totalled 500 ps, with 2500 coordinate sets saved for styrene, and 1000 ps, with 500 coordinate sets saved for *cis*-β-methylstyrene and *trans*-β-methylstyrene. In addition, the 4 MD trajectories for styrene were repeated with modified parameters for the torsion potentials associated with the allylic bonds, listed in Table I, to compare the effect of variation in key dihedral parameters on the simulations.

Analysis of Dynamics Simulations. Two geometric parameters were used as predictors of epoxidation of the substrate and were calculated for each structure stored during the course of the molecular dynamic simulations. The first property monitored was the distance between the C_β atom of the substrate and the ferryl oxygen. The C_β distance was chosen as a measure of reaction because of the greater stability of the benzylic radical formed when oxygen attacks at the C_β position rather than the C_α position. Each "snapshot" in which this distance was less than 4 Å was counted as an orientation leading to epoxidation. The chosen value of 4 Å is approximately 133% of the sum of the van der Waals radii of the carbon atom and the ferryl oxygen. This value is large enough to generate adequate statistical sampling of the trajectories while maintaining close proximity between the substrate and ferryl oxygen. For each such coordinate set that met this first criteria, the second geometric parameter was monitored; the angle corresponding to the direction of the C_α–C_β π orbitals with respect to the ferryl oxygen was calculated (Figure 1). This angle is the one between a vector (***V1***) from the C_β atom to the ferryl oxygen, and the normal (***N1***) to the plane of the C_α, C_β, and C methyl atoms. Values of this angle identify the preferred face for epoxide formation and hence the preferred epoxide stereoisomer. Values less than 80° correspond to formation of the 1*S*,2*R* epoxide and those greater than 100° to formation of the 1*R*,2*S* epoxide, for *cis*-β-methylstyrene (styrene). For *trans*-β-methylstyrene, values less than 80° correspond to the 1*R*,2*R* product and those greater than 100° correspond to the 1*S*,2*S* epoxide. Angles between 80° and 100° have been designated "σ" and correspond to an "edge-on" approach of the substrates that were considered to be unreactive or not specific toward epoxidation and were not counted in the prediction of enantiomeric excess.

Results

Oxidation of Styrene, *cis*-β-Methylstyrene, and *trans*-β-Methylstyrene. Incubation of styrene with a reconstituted cytochrome P450$_{cam}$ system yields styrene oxide and benzaldehyde as the major products and phenylacetaldehyde and one of the ring hydroxylated styrene isomers as very minor products (Table II). These and all the other products reported in this paper, with the exception of the ring hydroxylated isomers, were characterized by direct gas chromatographic and mass spectrometric comparison with authentic materials. The ring hydroxylated products had retention times consistent with ring hydroxylation and were characterized by gas chromatography–mass spectrometry, but the authentic isomers were not available for direct comparisons. Measurement of the turnover rates for the styrene metabolites shows that benzaldehyde is formed approximately three times as fast as styrene oxide, whereas phenylacetaldehyde and the ring hydroxylated product are formed at approximately one-tenth the rate of styrene oxide (Table II). The turnover rates of the trace products could not be accurately measured due to the low quantities in which they were formed. The turnover values cited in the table for these metabolites have been estimated from the ratio of the final integrated GLC peaks for the metabolite in question versus that for one of the major metabolites for which the turnover rate could be accurately measured. Control experiments without NADH show that formation of all the products is enzyme dependent. However, addition of catalase to the incubation decreases the formation of benzaldehyde without detectably altering the formation of the other products. This suggests that some, if not all, of the benzaldehyde formation is supported by H_2O_2 generated in situ. This inference is supported by the finding that benzaldehyde, but none of the other products, is obtained if NADH is replaced in the incubation by an amount of H_2O_2 equivalent to the amount normally produced in the incubation (~1 mM).

Table II. Turnover Rates for the Products Formed in the Oxidation of Styrene and *cis*- and *trans*-β-Methylstyrene by Cytochrome P450$_{cam}$

Substrate	Products (turnover rates in nmol/nmol cytochrome P450/min)[a]				
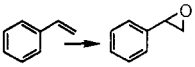	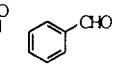			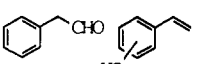	
1.1 ± 0.1	3.2 ± 0.3			0.09	0.09
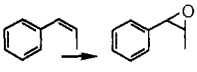	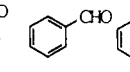			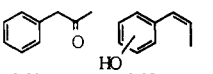	
0.54 ± 0.08	0.31 ± 0.03	0.12 ± 0.02		0.03	0.03
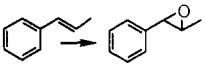	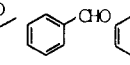	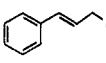		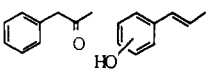	
0.15 ± 0.03	0.47 ± 0.04	0.06 ± 0.02		0.001	0.01

[a] Standard deviations from a minimum of three experiments are given for the major products. Turnover numbers for the trace products (benzaldehyde, 1-phenyl-2-propanone, and ring hydroxylated isomers) are estimated by peak height comparison to one of the major products.

Incubation of *cis*-β-methylstyrene with the reconstituted cytochrome P450$_{cam}$ system produces *cis*-β-methylstyrene oxide, *cis*-3-phenyl-2-propen-1-ol, and benzaldehyde as the major products, with 1-phenyl-2-propanone and a ring hydroxylated isomer of *cis*-β-methylstyrene as trace metabolites (Table II). Control experiments again establish that all the products are NADH and enzyme dependent and that benzaldehyde is, at least in part, the result of a side reaction between the olefin and endogenously generated H_2O_2. No *trans*-β-methylstyrene oxide was detected in these incubations. Oxidation of the olefin to the epoxide occurred five times faster than hydroxylation of the methyl group, and twenty times faster than formation of the two trace metabolites. Analogous incubation of *trans*-β-methylstyrene yields *trans*-β-methylstyrene oxide, benzaldehyde, and *trans*-3-phenyl-2-propen-1-ol as the major metabolites. 1-Phenyl-2-propanone and a ring-hydroxylated product are also obtained in much lower yields (Table II). The benzaldehyde is formed, as already noted, by reaction of the olefin with H_2O_2. Epoxidation of the *trans* olefin was substantially (4–7×) slower than epoxidation of either styrene or the *cis* olefin (Table II). Formation of the rearranged ketone and the ring-hydroxylated product was much slower than epoxidation of the *trans* double bond.

Stoichiometry of the Cytochrome P450$_{cam}$-Catalyzed Olefin Oxidations. The observation that benzaldehyde results from oxidation of the styrenes by endogenously generated H_2O_2 suggests that the turnover of these substrates is associated with substantial uncoupling of the epoxidation reaction from the consumption of

Table III. Stoichiometry of the Oxidation of Styrene and *cis*- and *trans*-β-Methylstyrene by Cytochrome $P450_{cam}$

substrate	rate (nmol/nmol of cytochrome P450/min)			
	NADH	O_2	H_2O_2	product[a]
styrene	51 ± 3	46 ± 2	53 ± 3	1.1 ± 0.2
cis-β-methylstyrene	55 ± 2	41 ± 5	56 ± 1	0.54 ± 0.08
trans-β-methylstyrene	32 ± 1	30 ± 8	29 ± 3	0.15 ± 0.03
camphor	260 ± 20	260 ± 10	9 ± 1	290 ± 10

[a] The product is the epoxide for the styrenes and 5-*exo*-hydroxycamphor for camphor. The rates of product formation from the olefins are slightly higher if the other metabolites are included, although benzaldehyde is not counted as a product for these purposes because it is produced by a peroxide-dependent reaction.

Table IV. Absolute Stereochemistry of the Epoxides of Styrene and *cis*- and *trans*-β-Methylstyrene Produced by Cytochrome $P450_{cam}$

substrate	stereoisomers	absolute stereochemistry	
		exptl	calcd
styrene	1*S*:2*R*	83:17	65:35
cis-β-methylstyrene	1*S*,2*R*:1*R*,2*S*	89:11	84:16
trans-β-methylstyrene	1*S*,2*S*:1*R*,2*R*	75:25	75:25

NADH. In order to evaluate the degree of uncoupling in these reactions, the consumption of NADH was measured spectroscopically, the consumption of oxygen with an oxygen electrode, the formation of H_2O_2 by a chemical assay, and the formation of substrate-derived metabolites by GLC (Table III). The plots used to determine the oxygen and NADH consumption rates were linear over the time course of the experiment. The hydroxylation of camphor, as previously reported,[25] is tightly coupled with no more than a trace of the catalytic turnover diverted to the production of H_2O_2 rather than 5-hydroxycamphor. In contrast, catalytic turnover of the three olefins is not only slower than is the turnover of camphor but also highly uncoupled (Table III). NADH and oxygen are consumed at about the same rates in the turnover of styrene and *cis*-β-methylstyrene but at slower rates in the turnover of *trans*-β-methylstyrene. The slightly lower values for oxygen than NADH consumption could be due to some reduction of oxygen to water, but are more likely due to a systematic error in the oxygen measurements because there is good agreement between the rates of NADH consumption and hydrogen peroxide formation. Thus, nearly all of the NADH consumed is used to reduce molecular oxygen to hydrogen peroxide rather than to oxidize the olefins, the oxidation of styrene oxide accounting for less than 2%, and the oxidation of the two β-methylstyrenes for less than 1%, of the catalytic turnover.

Absolute Stereochemistry of Olefin Oxidation. The *cis*- and *trans*-β-methylstyrenes are oxidized with retention of the olefin stereochemistry, in accord with earlier work on cytochrome P450-catalyzed olefin epoxidations.[26] Analysis of the epoxides on a chiral GLC column which fully resolves the stereoisomers shows that styrene is oxidized to an 83:17 (±2) ratio of the *S*:*R* enantiomers, *cis*-β-methylstyrene to an 89:11 (±2) ratio of the 1*S*,2*R*:1*R*,2*S* isomers, and *trans*-β-methylstyrene to a 75:25 (±3) ratio of the 1*S*,2S:1*R*,2*R* enantiomers (Table IV).

Computation Results. AM1 geometry optimizations resulted in planar structures for styrene and *trans*-β-methylstyrene. However, the lowest energy structure of *cis*-β-methylstyrene was calculated to be nonplanar about the C_ϕ–C_α bond with a dihedral angle of approximately 42° for τ (Figure 1). This nonplanarity is due to the steric repulsion between the methyl group and the phenyl ring. The barrier to rotation about τ, using AM1, is estimated to be approximately 1.5 kcal/mol for styrene and slightly higher for *cis*-β-methylstyrene.

(25) Atkins, W. M.; Sligar, S. G. *J. Am. Chem. Soc.* **1987**, *109*, 3754.
(26) (a) Watanabe, T.; Akamatsu, K. *Biochem. Pharmacol.* **1974**, *23*, 1079. (b) Watanabe, T.; Ueno, Y.; Imazumi, J. *Biochem. Pharmacol.* **1971**, *20*, 912. (c) Ortiz de Montellano, P. R.; Mangold, B. L.; Wheeler, C.; Kunze, K. L.; Reich, N. O. *J. Biol. Chem.* **1983**, *258*, 4202.

Table V. Interaction and Total Energies for the Docking of *trans*-β-Methylstyrene, *cis*-β-Methylstyrene, and Styrene in the Cytochrome $P450_{cam}$ Active Site

minimized orientation[a]	configuration[b]	interaction energy (*I*)[c]	substrate energy (*S*)[c]	sum[c] *I* + *S*	total[c]
	A. *trans*-β-Methylstyrene				
O1	1*R*,2*R*	−12.9	9.3	−3.6	−3287
O2	1*S*,2*S*	−16.3	8.2	−8.1	−3291
O3	1*S*,2*S*	−21.3	8.5	−12.8	−3296
O4	1*R*,2*R*	−22.6	6.8	−15.8	−3298
	B. *cis*-β-Methylstyrene				
O1	1*S*,2*R*	−19.2	9.2	−10.0	−3291
O2	1*R*,2*S*	−17.2	8.3	−8.8	−3292
O3	1*S*,2*R*	−17.9	9.8	−8.1	−3289
O4	1*R*,2*S*	−15.8	8.8	−7.0	−3285
	C. Styrene				
O1	1*S*	−17.5	5.3	−12.2	−3301
O2	1*R*	−15.5	5.5	−10.0	−3301
	D. Styrene (with Modified Dihedral Force Constants for the Out-of-Plane Angle)				
O1	1*S*	−17.5	6.8	−10.7	−3301
O2	1*R*	−15.5	10.5	−5.1	−3296

[a] The notation (O1, O2, O3, O4) is used to distinguish the differential orientations from each other and to correlate with the dynamics results presented in Table VI. [b] The stereochemistry of the expected epoxide product from each minimized orientation is listed using the nomenclature defined in the Methods section. [c] All energies in kcal/mol.

Radical stabilities for hydroxyl radical attack on the π system of *cis*-β-methylstyrene indicated the benzylic radical formed by attack at C_β was the most stable (by 9 kcal/mol), as was expected a priori. These results confirmed that the most likely site for attack is the C_β atom of the allylic system. Thus, the distance between the C_β and ferryl oxygen was chosen as an indicator of whether or not each snapshot recorded in the MD simulation is within a reactive distance.

Energy minimizations were performed for each initial orientation of each substrate, in an effort to find the most favorable binding mode for the substrate, and subsequently used as a starting point for molecular dynamic simulations. From the minimized complexes, the substrate–protein interaction energies for each optimized complex were determined. These interaction energies, as well as the total energies, are listed in Table V for *trans*-β-methylstyrene, *cis*-β-methylstyrene, and styrene, respectively. In this table, the first column ("O1", "O2", "O3", "O4") denotes the different orientation of the substrate in the protein binding site, while the second column lists the expected stereochemistry (e.g. 1*R*,2*R*) of the epoxide if the product were to be formed with the substrate in the corresponding minimized orientation. The interaction energy (*I*) is the sum of the nonbonded energy contributions between the substrate and the protein binding site. The substrate energy (*S*) is simply the internal energy of the substrate in the conformation minimized in the protein binding site for each orientation, and *I* + S, column 5, is the sum of these two energies as calculated by the ANAL program in AMBER. The final column in Table V lists the total minimized energy of the entire protein–substrate complex. All energies are reported in kcal/mol.

Table VI lists the results of the MD simulations, each trajectory corresponding to 125 ps. For each substrate, the first column in these tables gives a shorthand description of the initial conditions for each trajectory. The notation O1, O2, as in Table V, indicates the initial substrate orientation, while the added symbols V1 and V2 correspond to the two different initial velocity distributions used for each orientation. The second column, as in Table V, gives the predicted stereochemistry of the epoxide were it to be formed by the initial optimized substrate. The third column gives the total number of coordinate sets, out of 625 saved for each trajectory, in which the C_β atom of the substrate was within 4 Å of the ferryl oxygen. The last three columns list the number of coordinate sets with the specified range of values of ϕ (see Figure 1). These ranges of values correspond to the qualitatively different

Table VI. Results of Four Molecular Dynamics Simulations, Totaling 24 125 ps Trajectories for Styrene, *cis*-β-Methylstyrene, and *trans*-β-Methylstyrene

A. *trans*-β-Methylstyrene

simulation[a]	configuration[b]	total no.[c]	0–80° [d] 1*R*,2*R*	80–100° [d] σ	100–180° [d] 1*S*,2*S*
O1V1	1*R*,2*R*	208	105	27	76
O1V2	1*R*,2*R*	278	212	14	52
O2V1	1*S*,2*S*	173	71	17	85
O2V2	1*S*,2*S*	305	133	30	142
O3V1	1*S*,2*S*	202	82	30	90
O3V2	1*S*,2*S*	625	0	0	625
O4V1	1*R*,2*R*	591	2	6	583
O4V2	1*R*,2*R*	487	93	4	390
total		2869	698	128	2043
enantiomeric ratio: 1*S*,2*S*:1*R*,2*R* 75:25					

B. *cis*-β-Methylstyrene

simulation[a]	configuration[b]	total no.[c]	0–80° [d] 1*S*,2*R*	80–100° [d] σ	100–180° [d] 1*R*,2*S*
O1V1	1*S*,2*R*	26	3	5	18
O1V2	1*S*,2*R*	100	74	3	23
O2V1	1*R*,2*S*	187	187	0	0
O2V2	1*R*,2*S*	96	93	1	2
O3V1	1*S*,2*R*	103	103	0	0
O3V2	1*S*,2*R*	28	6	1	21
O4V1	1*R*,2*S*	6	0	0	6
O4V2	1*R*,2*S*	35	12	1	22
total		581	478	11	92
enantiomeric ratio: 1*S*,2*R*:1*R*,2*S* 84:16					

C. Styrene

simulation[a]	configuration[b]	total no.[c]	0–80° [d] *S*	80–100° [d] σ	100–180° [d] *R*
O1V1	1*S*	9	5	4	0
O1V2	1*S*	216	124	25	67
O2V1	1*R*	192	170	9	12
O2V2	1*R*	188	51	26	111
total		604	350	64	190
enantiomeric ratio: *S*:*R* 65:35					

D. Styrene (with Modified Dihedral Force Constants for the Out-of-Plane Angle)

simulation[a]	configuration[b]	total no.[c]	0–80° [d] *S*	80–100° [d] σ	100–180° [d] *R*
O1V1	1*S*	465	457	4	4
O1V2	1*S*	115	115	0	0
O2V1	1*R*	438	36	71	331
O2V2	1*R*	212	141	3	68
total		1230	749	78	403
enantiomeric ratio: *S*:*R* 65:35					

[a] The notation (O1, O2, O3, O4) labels the initial optimized orientation for each trajectory and has a 1:1 correspondence to the notation used in Table V. The two initial velocity distributions chosen for each minimized orientation are designated by a second label (V1, V2) for each trajectory. [b] Predicted stereoisomer of epoxide formed by the initial optimized complex. [c] Total number of stored structures out of 625 that had a C_β—O═Fe distance <4 Å. [d] The number of stored structures with C_β–O < 4 Å with this range of torsion angle values.

orientation of the substrate, with respect to the ferryl oxygen, and the distribution among them directly yields the overall enantiomeric ratios for epoxidation. Values between 80° and 100° were not counted in the calculated enantiomeric ratios. The second simulation for styrene listed in Table VI repeats the first styrene simulation but with the modified dihedral parameters listed in Table I (signified with asterisks). These simulations were performed to test for systematic changes in the predicted stereochemistry of epoxide formation due to the added torsional parameters for the substrates. While the second simulation results in twice as many coordinate sets within the cutoff distance of 4 Å, the distribution is very similar to the first set and leads to an identical prediction of stereochemistry. Therefore, the predictions appear to be relatively insensitive to the exact numerical value for the torsional parameter. The overall results from the dynamics simulations yield enantiomeric ratios of 75:25 (1*S*,2*S*:1*R*,2*R*) for *trans*-β-methylstyrene, 84:16 (1*S*,2*R*:1*R*,2*S*) for *cis*-β-methylstyrene, and 65:35 (1*S*,1*R*) for styrene (Tables IV and VI).

Discussion

Cytochrome $P450_{cam}$ catalyzes the oxidation of styrene, *cis*-β-methylstyrene, and *trans*-β-methylstyrene to the corresponding epoxides. The only epoxidation previously shown to be catalyzed by cytochrome $P450_{cam}$ is the conversion of 5,6-dehydrocamphor, the closest possible unsaturated analogue of camphor, to *exo*-5,6-epoxycamphor.[14c] The epoxide is the major enzyme-generated product from each of the three styrenes, although 3-phenyl-2-propen-1-ol, the product produced by ω-hydroxylation, is also obtained in significant amounts from the two β-methylstyrenes (Table II). The rates of formation of the ω-hydroxylated and epoxide products are comparable for *trans*-β-methylstyrene, but the terminal alcohol is formed at one-fifth the rate of the epoxide in the case of *cis*-β-methylstyrene. A trace of aromatic ring-hydroxylated product is obtained with all three styrenes, as is a trace of phenylacetaldehyde with styrene and 1-phenyl-2-propanone with the β-methylstyrenes. The aldehyde and ketone may arise by acid-catalyzed rearrangement of the epoxides or by direct formation from a cationic intermediate in the epoxidation process. Benzaldehyde is obtained as a major product in all three reactions, but control experiments show that benzaldehyde formation is largely peroxide dependent and is, therefore, primarily or exclusively produced by a mechanism other than normal enzyme-catalyzed turnover of the styrenes.

All three olefins are oxidized much less efficiently than camphor, the natural substrate, or 5,6-dehydrocamphor, the olefin analogue of camphor.[25,27] Under our conditions, NADH and oxygen are consumed approximately 5–6 times faster with camphor than with the olefins, and the hydroxylated product is produced more than a 100 times faster than the epoxides. In contrast to the reaction with camphor, which is tightly coupled and yields only traces of peroxide, oxidation of the olefin is highly uncoupled and produces much higher amounts of H_2O_2 than of the epoxides (Table III). Previous studies of substrate analogues that are less specifically bound by cytochrome $P450_{cam}$ than camphor have shown that decreasing the binding specificity decreases the hydroxylation regiospecificity and increases uncoupling.[11,12] The large degree of uncoupling with the styrenes suggests that they are loosely bound and can move about the active site with relative ease. This interpretation is supported by the molecular dynamics calculations, which show that the olefins spend a substantial fraction of the time with the double bond too far from the ferryl oxygen for epoxidation to occur. Of the 2500 molecular dynamic snapshots taken for styrene, the double bond was in a position to react with the ferryl oxygen in only 25% of them. Of the 500 snapshots taken for *cis*-β-methylstyrene and *trans*-β-methylstyrene, the double bond was in a position to react with the ferryl oxygen only 12% and 57% of the time, respectively. In contrast, molecular dynamics simulations of the binding of camphor to the active site of cytochrome $P450_{cam}$ suggest that it moves very little with respect to the heme, and the C_5-*exo* hydrogen atom is almost always within reactive distance to the ferryl oxygen.[27]

Remarkable agreement is obtained between the calculated and experimental ratios of the styrene and *cis*- and *trans*-β-methylstyrene epoxide enantiomers (Table IV). The dominant isomer in all instances has the *S* absolute configuration at the benzylic carbon. The calculations correctly predict the major isomer in all instances and result in values that are in excellent agreement for *cis* and *trans*-β-methylstyrene and reasonable agreement with styrene. The agreement between the simulations and experiment is very encouraging since these substrates are not oriented by polar interactions such as hydrogen bonds and are quite mobile in the binding site, and the product ratio is influenced by subtle steric interactions with the protein. The epoxidation stereochemistry

(27) Paulsen, M. D.; Ornstein, R. L. Abstract 283, 8th International Symposium on Microsomes and Drug Oxidations, Stockholm, Sweden, June 25–29, 1990.
(28) Collins, J. R.; Loew, G. H. *Int. J. Quantum Chem.: QBS* **1990**, *17*, 161.

for the three styrenes thus appears to be controlled by steric factors that are well modeled by molecular dynamics simulations.

Several important insights are obtained from the theoretical calculations. First, the relative energies of the optimized substrate–enzyme complexes alone cannot be used reliably to predict the correct product stereochemistry. As shown in Table V, using this criterion, the *trans*-β-methylstyrene would erroneously be predicted to preferentially form the 1*R*,2*R* epoxide. Even when the lowest energy orientation leads to the correct qualitative result, as for styrene and *cis*-β-methylstyrene, the energy differences between the orientations are quite small and, given the approximations and large number of degrees of freedom, cannot be used as reliable criteria. Finally, such criteria could not be used to predict the enantiomeric ratios obtained experimentally. Thus, MD simulations are needed to depict the interactions that modulate stereoselective product formation.

Additional, useful inferences can be deduced from the MD simulations themselves. One observation is that the dynamic behavior of low-energy structures that favor one enantiomer can lead to results that overwhelmingly favor the other one. This behavior is strikingly illustrated by orientation "O_4" of the *trans*-β-methylstyrene. The initial optimized structure favors the 1*R*,2*R* while the dynamic behavior favors the 1*S*,2*S* isomer. Another observation is that two orientations, each of which favors the same enantiomer, can have MD behavior leading to qualitatively different conclusions. For example, the two different minimized orientations of *trans*-β-methylstyrene, "O2" and "O3" that initially favor the 1*S*,2*S* enantiomer, lead to qualitatively different MD results. The dynamic behavior of orientation "O2" results in very little enantiomeric preference while that of orientation "O3" suggests that the reaction would proceed almost exclusively to the 1*S*,2*S* enantiomer. This result clearly illustrates the need to include several different starting orientations to reliably span possible modes of substrate–protein interactions. Further analysis of the two different trajectories of orientation 3 lead to the third instructive observation. Different initial velocity distributions can lead to qualitatively different conclusions. Therefore, in addition to several different orientations, multiple velocity distributions should also be used to ensure that the results are not unphysically biased.

Finally, it should be noted that none of the 8 different trajectories of 125 ps by itself gave the correct results for the enantiomeric product ratio of *cis*- and *trans*-β-methylstyrene. As can be seen from Table VI, it is only the total of these results that agree well with experiment. This result illustrates that multiple simulations must be performed to adequately sample the conformations and orientations available to the system and reliably predict product distributions when relatively short (125 ps) trajectories are used, even for a single site in a substrate with few conformational degrees of freedom. Carrying out the requisite multiple simulations was made possible by the use of a truncated model of the protein that corresponds to the well-defined, and relatively rigid, binding pocket of $P450_{cam}$. For other problems, where the entire protein must be used, it will be even more challenging to adequately sample the orientations and conformations available to the substrate and protein that lead to reliable predictions of stereospecificity. These results have important implications for future theoretical studies. Since it is not possible, a priori, to predict the number or length of the trajectories necessary to adequately sample phase space, other criteria must be used to assess the validity of the simulations. In the simulations presented here, the substrates showed multiple changes in orientation during the course of each trajectory, and the predictions are consistent with experiment for all three substrates without prior knowledge of the experimental results. These facts argue against fortuitous agreement and suggest that the simulations have adequately explored the relevant orientations available to the substrates. Adequate sampling can be expected for systems that follow ergodic dynamics, as appears to be the case with these substrates, but cases where the substrate motion is severely constrained by the protein would lead to the expectation that the methods outlined here would fail. The results presented here indicate that multiple simulations of moderate length are much more effective in exploring allowed substrate–enzyme orientations. Simulations comparing these methods with single nanosecond trajectories are in progress.

In order to understand the interactions leading to the observed stereochemical preference, we examined the nonbonded contacts between the protein binding site and the substrates. From the minimized complexes and MD results, three amino acids were identified as possibly playing a significant role in determining the product ratios. The methyl groups of Val295, Val396, and Thr252 were seen to interact quite strongly with the substrate, blocking formation of the disfavored enantiomer. Subsequent calculations using the identical protocols and procedures reported here of the mutant protein, V295A, V396A, and T252S with *cis*-β-methylstyrene resulted in enantiomeric ratios for 1*S*,2*R*:1*R*,2*S* of 55:45. These calculations support the hypothesis that these residues are indeed involved in the control of stereospecificity and indicate that other mutations may be identified in the binding site of $P450_{cam}$ that would actually reverse the enantiomeric ratios observed for the wild-type.

Acknowledgment. Support for this work by National Institutes of Health Grants GM 25515 (P.O.M.) and GM 29743 (G.H.L.) is gratefully acknowledged. We also thank the Pittsburgh Supercomputer Center, sponsored by the National Science Foundation, at which the computations were performed.